12-1-2011

Mechanical Characterization of Fourth Generation Composite Humerus

Prateek Grover
Medical College of Wisconsin

Carolyne Albert
Marquette University, carolyne.albert@marquette.edu

Mei Wang
Marquette University, mei.wang@marquette.edu

Gerald F. Harris
Marquette University, gerald.harris@marquette.edu

Accepted version. *Proceedings of the Institution of Mechanical Engineers, Part H: Journal of Engineering in Medicine*, Vol. 225, No. 12 (December 2011): 1169-1176. DOI.

Mechanical Characterization of Fourth Generation Composite Humerus

Prateek Grover, M.D., Ph.D. candidate
Medical College of Wisconsin
Milwaukee, WI
Marquette University
Milwaukee, WI

Carolyne Albert, Ph.D.
Medical College of Wisconsin
Milwaukee, WI

Mei Wang, Ph.D.
Medical College of Wisconsin
Milwaukee, WI
Marquette University
Milwaukee, WI

Gerald F. Harris, Ph.D., P.E.
Medical College of Wisconsin
Milwaukee, WI
Marquette University
Milwaukee, WI

Journal of Engineering in Medicine Proceedings of the Institution of Mechanical Engineers, Part H, Vol. 225, No. 12 (December 2011): pg. 1169-1176. DOI.

Abstract:

Mechanical data on upper extremity surrogate bones, supporting use as biomechanical tools, is limited. The objective of this study was to characterize the structural behavior of the fourth generation composite humerus under simulated physiologic bending, specifically, stiffness, rigidity, and mid-diaphysial surface strains. Three humeri were tested in four-point bending, in anatomically defined anteroposterior(AP) and mediolateral(ML) planes. Stiffness and rigidity were derived using load-displacement data. Principal strains were determined at the anterior, posterior, medial and lateral surfaces in the humeral mid-diaphysial transverse plane of one specimen using stacked rosettes. Linear structural behavior was observed within test range. Average stiffness and rigidity were greater in the ML (918+18 N/mm; 98.4+1.9 Nm^2) than the AP plane (833+16 N/mm; 89.3+1.6 Nm^2), with little interspecimen variability. The ML/AP rigidity ratio was 1.1. Surface principal strains were similar at the anterior (5.41 με/N) and posterior (5.43 με/N) gauges for AP bending, and comparatively less for ML bending, i.e., 5.1 and 4.5 με/N, at the medial and lateral gauges, respectively. The study provides novel strain and stiffness data for the fourth generation composite humerus, and adds to published construct rigidity data. ***Results support use of this composite bone as a tool for modeling and experimentation.***

Keywords: Adult human humerus; Composite material; Four**-**point bending; Surface strains; Construct stiffness and rigidity; Orthopaedic and rehabilitation applications.

1. INTRODUCTION

Composite (polymer and glass fiber) long bones, with standardized geometric and material properties, are frequently used as biomechanical tools to evaluate trauma fixation **[1]**, endoprosthesis **[2]**, arthroplasty **[3, 4]**, and other orthopaedic procedures**.** Composites have also been used to obtain standard, accessible and testable geometry for the development of finite element (FE) models of the femur **[5]** and tibia **[3]**. More detailed mechanical characterization of composite bones in terms of stiffness, flexural rigidity and strain distribution can add to the utility of these important biomechanical tools. Experimentally derived structural data also provide a resource to help in validation of corresponding FE models developed from these bones **[1,6,7,8,9]**. To date, the only upper extremity composite bones that have been characterized to some extent are the third and fourth generation (Sawbones, Pacific Research

Labs, WA, USA) composite humeri **[10]**. The goal of the present study is to provide new information and detail on strain characterization of the fourth generation composite humerus under simulated physiological bending.

The specific geometry of the composite humerus (Sawbones, Pacific Research Labs, WA, USA) has been derived from CT scans of a Caucasian male cadaver. Material properties of the outer composite short fiber reinforced epoxy cortex, and inner polyurethane foam cancellous layer have been modified over the past two decades to more closely approximate human bone mechanical properties. The most recent modifications are represented by the fourth generation models. Advantages of composite models include consistent geometry and material properties with very low interspecimen variability. Hence, fewer specimens can be used, with greater confidence in the repeatability of results. The more stringent usage and preservation requirements associated with cadaveric bone testing are also avoided **[11]**. Previous studies of composite long bones include second **[11,12,13]**, third **[3,4,5,14]**, and fourth **[15,16]** generation femur and tibia, which have been tested in bending, torsion and axial compression. Structural parameters obtained from tests of the tibia and femur models include stiffness [**5,11,12,14,16**], rigidity **[5,14,16]**, and strain behavior **[4,12,13,16]**. To date, the fourth generation composite humerus has been tested in bending and torsion for torsional stiffness, flexural rigidity and strength **[10].** Strain characterization for this composite bone has not been reported.

The humerus experiences bending loads and moments at the shoulder and elbow during activities of daily living **[17]**. Shoulder moments reported for physiologic activities include 16 Nm for the sit-to-stand maneuver, 12 Nm for stand-to-sit, and a range of 22-28 Nm for lifting objects **[18]**. Mobility aid assisted moments have also been reported, including a 24 Nm shoulder moment for cane assisted walking **[18]**, and moment range 4.1-11.3 Nm at the shoulder and 0.5-7.9 Nm at the elbow for low intensity wheelchair propulsion **[19]**. Higher intensity wheelchair tasks can impose greater moments, with a range of 24-70 Nm (shoulder) and 8-51 Nm (elbow) for weight relief lift in a wheelchair; and 36-97 Nm (shoulder) and 32-75 Nm (elbow) for negotiating a curb in a wheelchair **[19]**. Humeral bending

moments to failure average approximately 155 and 84 Nm for males and females, respectively **[20]**.

The objective of this study was to characterize the structural behavior of the fourth generation composite humerus, in terms of construct stiffness and rigidity, and mid-diaphysial surface strains at the anterior, posterior, medial and lateral surfaces under simulated physiologic bending.

2. MATERIALS AND METHODS

Fourth-generation composite humeri (HS4, Model 3404, Pacific Research Labs Inc., VA, USA) were tested in a four-point bending configuration. Stiffness data were collected using three HS4, while detailed mid-diaphysial surface strain data were collected from a single strain-gauged specimen.

2.1 Biomechanical Evaluation

Anatomic planes were identified for the composite humerus (Figure 1). The mid-diaphysial transverse (T) plane was defined as perpendicular to the humeral shaft axis. The anteroposterior (AP) and mediolateral (ML) planes were defined orthogonal to the T plane. The ML plane passed through the medial surface and sharp lateral border, aligned with the transepicondylar axis **[21]**. The AP plane passed through the posterior surface and mid-humeral anterior border. Four stacked rectangular rosettes (C2A-06-062WW-350, Vishay Micro-Measurements, NC, USA) were lined up in the T plane, 190 mm from the proximal end of the specimen. The anterior (A) and posterior (P) gauges were located in the AP plane, and medial (M) and lateral (L) gauges in the ML plane, on corresponding aspects of the mid-diaphysis. The central strain gauge (II) in all four rosettes was aligned with the shaft of the humerus. The gauges were then bonded to the specimen with cyanoacrylate, M-bond 200 (Vishay Micro-Measurements, NC, USA).

Figure 1. *Four- point bending test configuration of strain-gauged fourth generation sawbones humerus in AP and ML bending, with location of strain-gauges on the specimen, and on the cross-section in the mid-diaphysial transverse (T) plane.*

Journal of Engineering in Medicine Proceedings of the Institution of Mechanical Engineers, Part H, Vol. 225, No. 12 (December 2011): pg. 1169-1176. DOI.

A four-point load configuration was chosen to ensure pure bending, zero shear, and a constant moment throughout the mid diaphysis between the inner supports. The bending tests were performed with a servo hydraulic material testing system (MTS 809, Eden Prairie, MN), with integrated load cell and linear variable displacement transducer. The test setup was comprised of two cylindrical superior load rollers spaced 56 mm apart and two cylindrical inferior support rollers spaced 184 mm apart (L). The support roller was 64 mm from the loading roller on each side (C). ***This distance between the outer and inner rollers (C), was chosen based upon the most stable configuration of the humerus during testing, while being closest to one third of the L, for consistency with other reported work [11,12,15,16]. A stable configuration implied that the humerus did not rotate visibly, while being tested in four-point bending without any additional constraints. Three specimens, one of which was instrumented with strain gauges, were subjected to three cycles of loading and unloading in the AP and ML planes at a frequency of 0.2 Hz, that was equivalent to a loading rate of approximately 0.18 mm/sec. The first two cycles were meant to precondition the specimens***. Load-displacement data were collected at 200 Hz. The tests were performed without additional constraints, up to a maximum compression of 500 N (equivalent moment 16 Nm). Following gauge calibration, strain data were collected from the instrumented specimen for 3 trials each of AP and ML four-point bending to a maximum load of 400 N (moment 12.8 Nm). For both stiffness and strain data collection, the anterior and medial surfaces were under tension during AP and ML bending, respectively.

2.2 Data Analysis

Stiffness (S) in the AP and ML planes was calculated as the slope of the force-deflection curve of the third cycle.

Flexural rigidity (EI), a measure of extrinsic stiffness, was approximated by the fundamental beam formula (2.1), that relates specimen rigidity to specimen stiffness and test configuration specific measures, namely, the distance between

two support rollers, L and distance between the outer and inner rollers, C.

$$EI = \frac{S}{12}[C^2(3L - 4C)] \qquad (2.1)$$

The flexural rigidity formula for the present study (2.2) was derived from (2.1), by using specimen stiffness, S and test configuration specific parameters (L = 184.0 mm, C = 64.0 mm), illustrated pictorially in Figure 1.

$$EI = \frac{4.625}{12}SC^3 \qquad (2.2)$$

This formula is similar to that used by other researchers [10,15].

Authors of the present study calculated test configuration-specific stiffness, S for Dunlap et al [10] by using their reported rigidity data, EI and configuration-specific rigidity formula (2.3)

$$EI = \frac{4.59}{12}SC^3 \qquad (2.3)$$

Strains: Strains from the three gauges of each stacked rectangular rosette (ε_I, ε_{II}, and ε_{III}) were converted into principal strains (ε_1 and ε_2), using standard strain transformation formulae for plane stress [22], equations (2.3), (2.4):

$$\varepsilon_1 = 0.5\,(\varepsilon_I + \varepsilon_{III}) + 0.5[(\varepsilon_I - 2\,\varepsilon_{II} + \varepsilon_{III})^2 + (\varepsilon_{III} - \varepsilon_I)^2]^{0.5} \qquad (2.3)$$

$$\varepsilon_2 = 0.5\,(\varepsilon_I + \varepsilon_{III}) - 0.5[(\varepsilon_I - 2\,\varepsilon_{II} + \varepsilon_{III})^2 + (\varepsilon_{III} - \varepsilon_I)^2]^{0.5} \qquad (2.4)$$

where ε_1 and ε_2 are maximum principal (maximum tensile) and minimum principal (maximum compressive) strains, and ε_I, ε_{II} and ε_{III} are strains collected from the three gauges of the rosette.

Principal strains were evaluated over the test load range. Multiple samples were collected at specific load levels ranging from 100 N to 400 N for 3 trials, in order to assess inter-trial strain variability. A linear regression was done to describe the relationship between strain and applied loads.

Journal of Engineering in Medicine Proceedings of the Institution of Mechanical Engineers, Part H, Vol. 225, No. 12 (December 2011): pg. 1169-1176. DOI.

3. RESULTS

3.1 Stiffness and Flexural Rigidity

The three specimens showed similar load-displacement behavior in the test range. ***Preliminary testing demonstrated limited hysteresis for the specimens. The two preconditioning cycles were adequate to achieve consistent load-deformation results.*** Interspecimen variability in stiffness was small, with standard deviations (SD) of 1.9% for AP and 2.0% for ML bending. A linear trend in displacements versus force was observed, with R^2 values greater than 0.999. At a common displacement of 0.5 mm, the mean forces were 416.5 N and 459.0 N for AP and ML bending, respectively. The average stiffness was 832.9 (SD 16) N/mm in the AP plane and 917.6 (SD 18) N/mm in the ML plane. Mean rigidity in the AP and ML planes was 84.1 (SD 1.5) Nm^2 and 92.7 (SD 1.8) Nm^2, respectively. The specimens were an average of 10.1 % stiffer in the ML plane than the AP plane. A representative load-displacement plot from one specimen is illustrated in Figure 2.

Figure 2. *Representative load-displacement plot of a 4th Generation sawbones humeri in AP and ML 4-point bending.*

3.2 Principal Strains

Collected strain data were greater in magnitude at the central strain gauge (ε_{II}), compared with the other two gauges of the rosette (ε_{I}, ε_{III}). This (ε_{II}) strain represented greater than 95% of the calculated maximum tensile and compressive strains. The maximum principal strains occurred at the tensile surface, at the A gauge for AP bending and M gauge for ML bending. Minimum principal strain was seen at the compressive surfaces, at the P gauge for AP bending and L gauge for ML bending. An excellent linear fit between strain and applied load was noted at the gauges in the plane of loading (A and P gauges for AP bending, and M and L gauges for ML bending), with R^2 values exceeding 0.99.

Figure 3*. Maximum (ε_1) and minimum(ε_2) principal strains over the load range 0-400 N.*

The relationship between maximum (compressive and tensile) strains and applied load was described as a slope, Figure 3. In the AP four-point bending tests, the slopes were 5.43 $\mu\varepsilon$/N at the A gauge and 5.41 $\mu\varepsilon$/N at the P gauge. The ML four-point bending test slopes were

Journal of Engineering in Medicine Proceedings of the Institution of Mechanical Engineers, Part H, Vol. 225, No. 12 (December 2011): pg. 1169-1176. DOI.

5.10 με/N at the M gauge and 4.50 με/N at the L gauge. Inter-trial strain variability at four load levels was evaluated. The mean coefficient of variance (CoV) for all gauges was 0.041 (SD 0.036). The smallest mean CoV for all gauges was seen at 100 N (Mean 0.036; SD 0.011), followed by 300 N (Mean 0.04; SD 0.03). The mean CoV was largest at 200 and 400 N (Mean 0.043; SD 0.05). Average CoV was greater in the ML plane (Mean 0.057; SD 0.043) compared with AP plane (Mean 0.024; SD 0.013).

In order to confirm the batch consistency of our specimen testing, a second strain gauge- instrumented specimen was tested. The anterior (A) and medial (M) strain-to-load slopes were identical. The posterior (P) slopes varied by less than 1%, and the lateral (L) by less than 4%.

4. DISCUSSION

The fourth generation composite humerus demonstrates linear behavior in AP and ML four-point bending for both displacement and maximum compressive and tensile strains (versus force). Slopes of maximum strains per unit force at the A (tensile) and P (compressive) gauges differ by less than 0.5%; the M gauge (tensile) value is greater than the L (compressive) by approximately 10%. It can be inferred that the neutral bending axis coincided with a point approximately midway between the A and P gauges in AP bending. In ML bending, the bending axis was located closer to the M gauge. The model was 10% stiffer in ML bending than in AP bending. Correspondingly, maximum tensile and compressive strains (per unit force) in ML bending were 6% and 17% lower than in AP bending (Figure 3). The slightly greater ML diameter (Figure 1), leading to a greater moment of inertia about the neutral (bending) axis was consistent with the lower ML bending strain.

Greater ML rigidity than AP rigidity has been reported for the fourth generation humerus [10]. While AP rigidity in the current study agreed closely (within 2%) with published results, ML rigidity was approximately 18% lower. In the current work, the specimens were constrained in the loading plane only. ***This less constrained configuration was chosen to better approximate humeral load conditions during assistive device-aided upper extremity motion as demonstrated in previous studies [23,24,25].*** Although the out-of-plane rotation was not constrained, no rotation

Journal of Engineering in Medicine Proceedings of the Institution of Mechanical Engineers, Part H, Vol. 225, No. 12 (December 2011): pg. 1169-1176. DOI.

was visually observed. In contrast, the other study's test configuration did not allow specimen rotation and translation.

Test specific stiffness was calculated from rigidity reported by Dunlap et al [10], using their rigidity formula. It is emphasized that stiffness is a function of the test configuration, in addition to specimen properties such as geometry and material properties. Configuration parameters influencing stiffness include the distance between inner and outer rollers, C and motion constraints. While a higher stiffness was obtained for the present study, and could be explained by the factors mentioned above, a direct comparison in stiffness values between the two studies is not possible.

Table 1*. Literature review of adult human humerus material properties*

Results from the current study are also contrasted with literature on human cadaveric humeral mechanical properties (Table 1). Only one study reported displacements **[26]**, in the range 1.2-1.5 mm, under a 7.5 Nm cantilever bending moment. For the current study, at an equivalent bending moment of 7.5 Nm, displacement was 0.28 mm in the AP plane and 0.25 mm in the ML plane. However, these results from the two studies are not directly comparable, since displacement is test setup dependent, and the two studies have very different loading configurations. Mean stiffness in four point bending, averaged in four planes, has been reported as approximately 1050 N/mm [27]. A lack of consensus exists as to the stiffer anatomic plane for cadaveric humeri, with literature reporting comparatively greater stiffness in the AP [28] as well as ML planes [29]. The rigidity results ranged from 90.9 [29] - 130.6 Nm [28] in the AP plane and 118.4 [28] - 138.5 Nm [29] in the ML plane. Composite bone studies [10] including the present study, reported rigidity that lay within those ranges from cadaveric studies. A comparison of rigidity between paired right and left humeri showed no significant difference [21,30]. However, greater mean stiffness for the left humeri has also been reported [29]. The cadaveric studies demonstrated 36% (ML bending) – 50% (AP bending) SD in rigidity [29], compared to a maximum 2% (current study) -10% [10] for composite humeral studies.

The calculated mean ML/AP rigidity ratio was approximately 0.7 for Lin *et al.* [28], 1.1 for the current study, 1.33 for the fourth

generation humerus [10], 1.5 for Henley *et al.* [29] and 1.6 for the third generation humerus [10]. However, taking the large standard deviations into consideration, the cadaveric results could vary from 0.3 [28] – 4.3 [29]. These differences in ML/AP ratios could be attributed in part to dissimilar cross-sectional geometry and material properties. Additional contributory factors consist of anatomic segment of the bone tested, loading constraints, and test configurations, including four-point bending for composite bones [10], and three-point bending [29], and cantilever testing [2121,28] for cadaveric bone. Nonetheless, the composite bone data lie well within the range for cadaveric studies.

Among the major composite long bones (Sawbones Worldwide, Pacific Research Labs, VA, USA), femurs are most rigid, followed by tibia, and then the humerus. While the third and fourth generation femurs are more rigid in their AP plane, the third and fourth tibias are more rigid in their ML plane. Rigidity in AP plane for the fourth generation femur and tibia is approximately 2.5 and 2.0 times that of the HS4 humerus, respectively In the ML plane, the rigidity of these femur and tibia is approximately 3.0 and 1.5 times that of the HS4 [16]. As weight bearing bones, the femur and tibia have a greater cross-sectional area and probably greater cortical thickness, compared with the humerus. Greater fourth generation material moduli make the fourth generation bones stiffer than their corresponding third generation counterparts. Mean bending stiffness reported for the second and third generation femur and tibia [11,12,14] are also much lower than the HS4.

The material structure of the HS4 is comprised of an outer cortical layer made of short fiber-reinforced epoxy, and an inner cancellous layer made of rigid polyurethane foam. Whereas the exact material composition is proprietary, the material properties have been documented by the manufacturer [3131]. The simulated cortical bone has a tensile modulus and strength of 16.0 GPa and 106 MPa, respectively. The respective compressive modulus and strength are 16.7 GPa and 157 MPa. The cancellous layer has a density of 0.27 g/cc, and compressive modulus and strength of 155 MPa and 6 MPa, respectively. Because the cancellous layer is thin, located closer to the neutral bending axis, and has much lower elastic modulus, the structural bending behavior in the test region of the diaphysis is principally determined by the outer cortical layer.

Journal of Engineering in Medicine Proceedings of the Institution of Mechanical Engineers, Part H, Vol. 225, No. 12 (December 2011): pg. 1169-1176. DOI.

The study provides mechanical characterization of the fourth generation composite humerus, including principal strains and stiffness in bending, which have not been published previously in literature. Mid-diaphysial surface principal strain and whole bone stiffness data have been determined specific to anatomic planes of bending, under physiologic loading. ***Stiffness and rigidity show minimal interspecimen variability. This agrees well with published literature. The ML/AP rigidity ratio has been found to lie within the ranges reported for the cadaveric humeri, although it does not correspond to a central value. Results from the current study support further the current use of the composite fourth generation humerus for biomechanical testing.*** These findings can also be useful for the development of humeral models employing finite element methods [5, 13].

Shortcomings from the current study are those of limited sample size (3 specimens: stiffness, rigidity; 2 specimen: principal strains), specificity of load configuration and constraints, and limited region of strain characterization (mid-diaphysis). Results from our tests show minimal batch variability. Tests from other batches may yield differing results. According to the manufacturer, the cortical modulus and strength may vary + 10%, while the geometry may vary + 0.1%. (Personal communication, Amy Johnson, M.S., Biomechanical Engineer, Pacific Research Labs, Vashon, WA, USA.)

CONCLUSION

Stiffness, rigidity, and mid-diaphysial strains of fourth generation composite humerus have been characterized in bending. Four-point bending tests were performed in AP and ML planes to simulate physiologic load conditions. Interspecimen standard deviation in stiffness was no greater than 2%. Rigidity results were similar to those reported in other composite bone and cadaveric humerus studies. The ML/AP rigidity ratio was within ranges calculated for cadaveric studies. The fourth generation composite humerus could be used as a reliable tool in experimental and modeling biomechanical studies.

Journal of Engineering in Medicine Proceedings of the Institution of Mechanical Engineers, Part H, Vol. 225, No. 12 (December 2011): pg. 1169-1176. DOI.

ACKNOWLEDGEMENTS

This work was supported by the NIDRR ARRT grant H133P080005 and NIDRR RERC on Technologies for Children with Orthopaedic Disabilities H133E100007.

The authors would like to acknowledge Linda McGrady, B.S., for assistance in data collection and analysis.

CONFLICT OF INTEREST STATEMENT

The authors declare that they have no conflict of interest. No benefits in any form have been or will be received from a commercial party related directly or indirectly to the subject of this manuscript.

REFERENCES

1. **Gardner, M.J., Griffith, M.H., Demetrakopoulos, D., Brophy, R.H, Grose, A., Helfet, D.L.,** and **Lorich, D.G.** Hybrid locking plating of osteoporotic fractures of the humerus. *Journal of Bone and Joint Surgery American*, 2006, 88(9), 1962-1967.

2. **Theilen, T., Maas, S., Zuerbes, A., Waldmann, D., Anagnostakos, K.,** and **Kelm, J.** Mechanical behavior of standardized, endoskeleton-including hip spacers implanted in composite femur. *International Journal of Medical. Sciences*, 2009, **6 (5)**, 280-286.

3. Completo, A., Fonseca, F., and Simoes, J.A. Finite element and experimental cortex strains of intact and implanted tibia. *Journal of Biomechanical Engineering*, 2007, **129 (5)**, 791-797.

4. **Completo, A., Fonseca, F., and Simoes, J.A.** Experimental validation of intact and implanted distal femur finite element models. *Journal of Biomechanics,* 2007, **40 (11**), 2467-2476.

5. **Papini, M., Zdero, R., Schemitsch, E.H.,** and **Zalzal, P.** The biomechanics of human femurs in axial and torsional loading: comparison of finite element analysis, human cadaveric femurs, and synthetic femurs. *Journal of Biomechanical Engineering*, 2007, **129 (1)**, 12-19.

6. **Anderson, A.E., Ellis, B.J.,** and **Weiss, J.A.** Verification, validation and sensitivity studies in computational biomechanics. *Computer Methods in Biomechanics and Biomedical Engineering,* 2007, **10 (3)**, 171-184.

7. **Cristofolini, L., Schileo, E., Juszczyk, M., Taddei, F., Martelli, S.,** and **Viceconti, M.** Mechanical testing of bones: the positive synergy of finite-element models and in-vitro experiments *Philos. Transact. A. Math. Phys. Eng. Sci.*, 2010, **368 (1920)**, 2725-2763.

8. **Henninger, H.B., Reese, S.P., Anderson, A.E.,** and **Weiss, J.A.** Validation of computational models in biomechanics. *Proc. IMechE, Part H: J. Engineering in Medicine*, 2010, **224 (7)**, 801-812.

9. **Viceconti, M., Olsen, S., Nolte, L.P.,** and **Burton, K.** Extracting clinically relevant data from finite element simulations. *Clinical Biomechanics*, 2005, **20 (5)**, 415-454.

10. **Dunlap, J.T., Chong, A.C.M., Lucas, G.L.,** and **Cooke, F.W.** Structural properties of a novel design of composite analogue humeri models. *Annals of Biomedical Engineering*, 2008, **36 (11)**, 1922-1926.

11. **Cristofolini, L.,** and **Viceconti, M.** Mechanical validation of whole bone composite tibia models. *Journal of Biomechanics,* 2000, **33 (3)**, 279-288.

12. **Cristofolini, L., Viceconti, M., Cappello, A.,** and **Toni, A.** Mechanical validation of whole bone composite femur models. *Journal of Biomechanics*, 1996, **29 (4)**, 525-535.

13. **Gray, H.A., Zavatsky, A.B., Taddei, F., Cristofolini, L.,** and **Gill, H.S.** Experimental validation of a finite element model of a composite tibia. *Proc. IMechE, Part H: J. Engineering in Medicine*, 2007, **221(3)**, 315-324.

14. **Heiner, A.D.,** and **Brown, D.B.** Structural properties of a new design of composite replicate femurs and tibias. *Journal of Biomechanics*, 2001, **34 (6)**, 773-781.

15. **Gardner, M.P., Chong, A.C.M., Pollock, A.G.,** and **Wooley, P.H.** Mechanical evaluation of large- size fourth- generation composite tibia and femur models. *Annals of Biomedical Engineering*, 2010, **38 (3)**, 613- 620.

16. **Heiner, A.D.** Structural properties of fourth-generation composite femurs and tibias. *Journal of Biomechanics*, 2008, **41 (15)**, 3282-3484.

17. **Dalton, J.E., Salkeld, S.L., Satterwhite, Y.E.,** and **Cook, S.D.** A biomechanical comparison of intramedullary nailing systems for the humerus. *Journal of Orthopaedic Trauma*, 1993, **7 (4)**, 367-374.

18. **Anglin, C.,** and **Wyss, U.P.** Arm motion and load analysis of sit-to-stand, stand-to-sit-cane walking and lifting. *Clinical Biomechanics*, 2000, **15 (6)**, 441-448.

19. **Van Drongelen, S., van der Woude, L.H., Janssen, T.W., Angenot, E.L., Chadwick, E.K.,** and **Veeger, D.J.H.** Mechanical load on the upper extremity during wheelchair activities. *Archives of Physical Medicine and Rehabilitation*, 2005, **86 (6)**, 1214-1220.

20. **Kirkish, S.L., Begeman, P.C.,** and **Paravasthu, N.S.** Proposed provisional reference values for the humerus for evaluation of injury potential. *SAE Transactions,* 1996, **105,** Paper 962416.

21. **Delude, J.A., Bicknell, R.T., Mackenzie, G.A., Ferreira, L.M., Dunning, C.E., King, G.J., Johnson, J.A.,** and **Drosdowech, D.S.** An anthropometric study of the bilateral anatomy of the humerus. *Journal of Shoulder and Elbow Surgery*, 2007, **16 (4)**, 477-483.

22. **Boresi, A.P.,** and **Schmidt, R.J.** Advanced mechanics of materials. 6th Ed., John Wiley and Sons, 2003, 811 pp.

23. **Slavens, B.A., Sturm, P.F., Bajournaite. R.** and **Harris, G.F.** Upper extremity dynamics during Lofstrand crutch-assisted gait in children with myelomeningocele. *Gait and Posture*, 2009, **30(4)**, 511-7.

24. **Konop, K.A., Strifling, K.M., Wang, M., Cao, K., Schwab, J.P., Eastwood, D., Jackson, S., Ackman, J.D.** and **Harris, GF.** A biomechanical analysis of upper extremity kinetics in children with cerebral palsy using anterior and posterior walkers. *Gait and Posture*, 2009, **30(3)**, 364-9.

25. **Strifling, K.M., Konop, K.A., Wang, M.** and **Harris, G.F.** Comparison of upper extremity glenohumeral joint forces in children with cerebral palsy using anterior and posterior walkers. *Biomedical Sciences Instrumentation,* 2009, **45**, 304-9.

26. **Fuchtmeier, B., May, R., Hente, R., Maghsudi, M., Volk, M., Hammer, J., Nerlich, M.,** and **Prantl, L.** Proximal humerus fractures: A comparative biomechanical analysis of intra and extramedullary implants. *Archives of Orthopaedic Trauma Surgery*, 2007, **127 (6)**, 441-447.

27. **Verbruggen, J.P.A.M., Sternstein, W., Blum, J., Rommens, P.M.,** and **Stapert, J.W.J.L.** Compression-locked nailing of the humerus. *Acta Orthopaedica*, 2007, **78 (1)**, 143-150.

28. **Lin, J., Inoue, N., Vadevit, A., Hang, Y.S., Hou, S.M.,** and **Chao, E.Y.S.** Biomechanical comparison of antegrade and retrograde nailing of humeral shaft fracture. *Clinical Orthopaedics and Related Research*, 1998, **351 (1)**, 203-213.

29. **Henley, M.B., Monroe, M.,** and **Tencer, A.F.** Biomechanical comparison of methods of fixation of a midshaft osteotomy of the humerus. *Journal of Orthopaedic Trauma,* 1991, **5 (1)**, 14-20.

30. **Zimmerman, M.C., Waite, A.M., Deehan, M.,** and **Oppenheim, W.** A biomechanical analysis of four humeral fracture fixation systems. *Journal of Orthopaedic Trauma*, 1994, **8 (3)**, 233-239.

31. ***http://www.sawbones.com/products/bio/composite.aspx***

32. **Elfick, A.P., Bedi, G., Port, A.,** and **Unsworth, A.** Design and validation of a surrogate humerus for biomechanical testing. *Journal of Biomechanics*, 2002, **35 (4)**, 533-536.

LIST OF FIGURES AND TABLES

Figure Captions

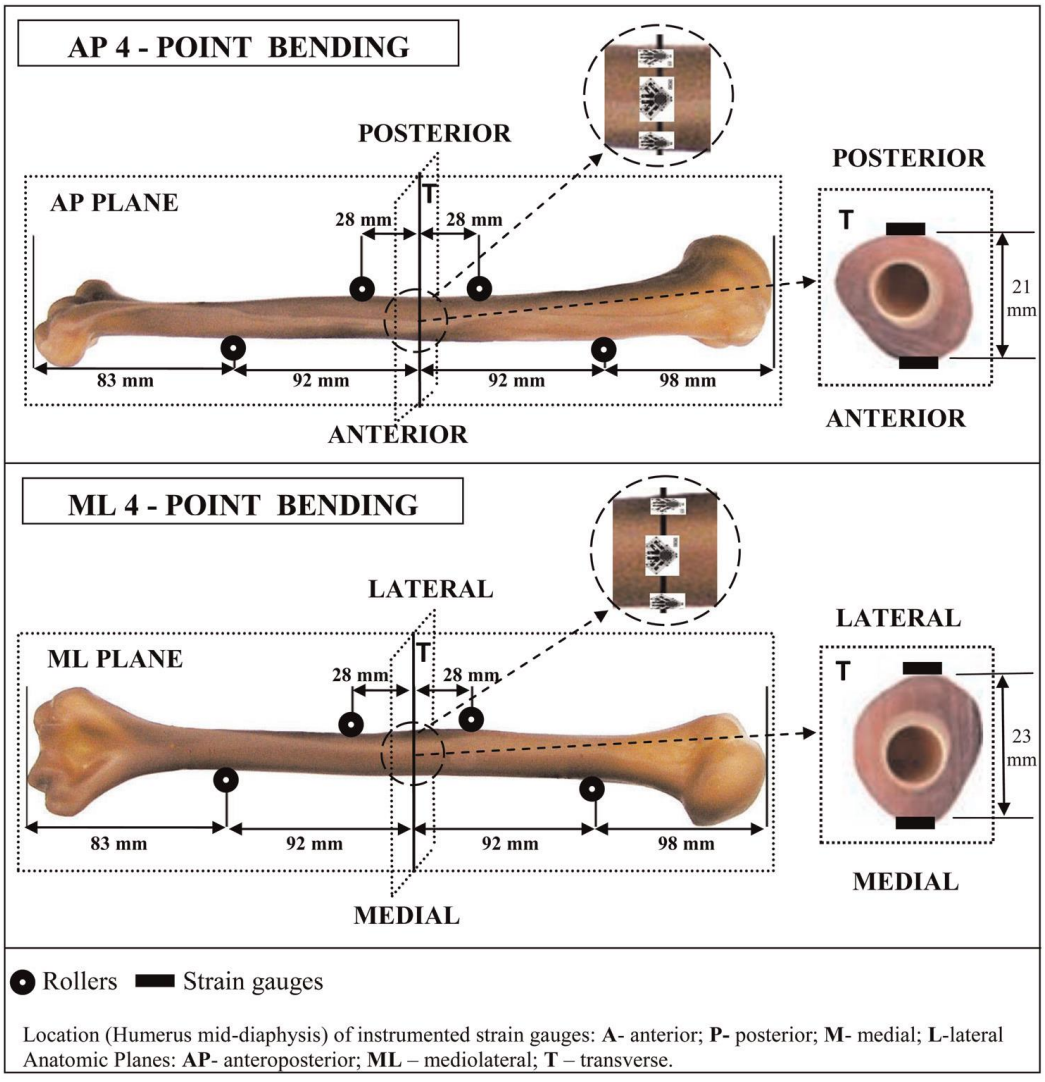

Figure 1. Four- point bending test configuration of strain-gauged fourth generation sawbones humerus in AP and ML bending, with location of strain-gauges on the specimen, and on the cross-section in the mid-diaphysial transverse (T) plane.

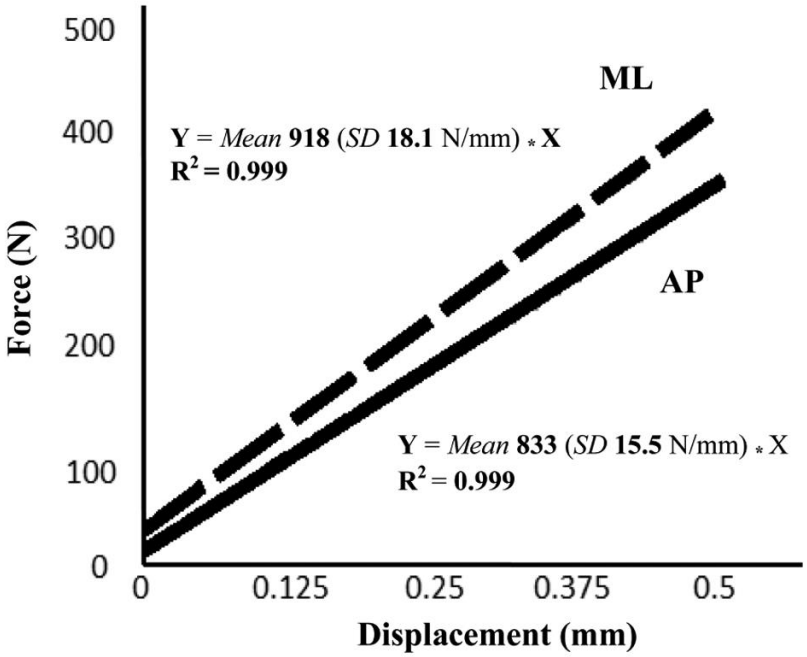

Figure 2. Representative load-displacement plot of a fourth generation sawbones humeri in AP and ML 4-point bending.

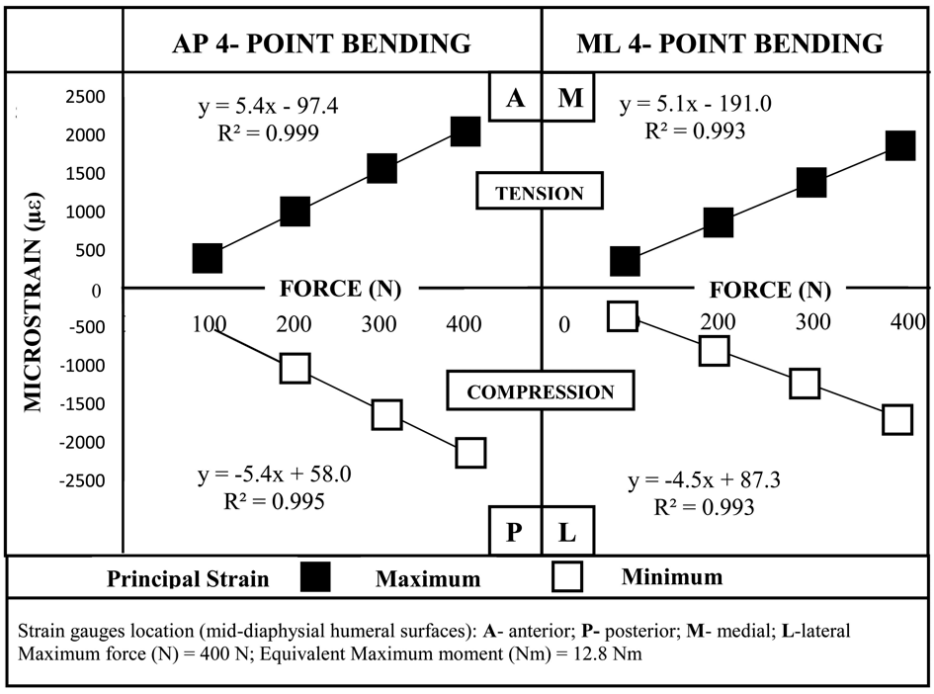

Figure 3. Maximum (ε_1) and minimum(ε_2) principal strains over the load range 0-400 N.

Journal of Engineering in Medicine Proceedings of the Institution of Mechanical Engineers, Part H, Vol. 225, No. 12 (December 2011): pg. 1169-1176. DOI.

Tables

Study	Specimen	Test	Moment (Nm)	AP plane		ML plane		Rigidity ratio
				Stiffness (N/mm)	Rigidity (Nm^2)	Stiffness (N/mm)	Rigidity (Nm^2)	ML/AP‡
Current study	4GC	1	16	832.9(15.5) (R^2 = 0.999)	84.1(1.5)	917.6(8.1) (R^2 = 0.999)	92.7(1.8)	1.1
[10]	4GC	1	Failure	204.8*	85.6(8.5)	272*	113.7(3.4)	1.3
[10]	3GC	1	Failure	141*	59.2(9.3)	226*	94.6(2.1)	1.6
[28]	Cad	2	1.4	285.5(123.3)	130.6(56.4) †	259(121)	118.4(56.4) †	0.9 [0.3–2.4]
[29]	Cad	3	n/a	L:10.1(5.2) R:8.2(3.8)	90.9(46.8) †	L:15.4(5.8) R:12.3(1.8)	138.6(52.2) †	1.5 [0.6–4.3]
Study	Specimen	Test	Moment (Nm)	Test plane not specified				L/R
[26] §	Cad	3	7.5	Deformation = 1.2–1.5 mm				1
[27] §	Cad	1	15	Stiffness = 1050 N/mm (average of four planes)				n/a
[30] §	Cad	1	5	n/a				1

Table 1. Literature review of adult human humerus material properties.

About the Authors

Prateek Grover, M.D., Ph.D. candidate : Orthopaedic and Rehabilitation Engineering Center, Marquette University, ASF, Suite 105, 735 N. 17th St, PO Box 1881, Milwaukee, WI 53201-1881, USA

Telephone:001-414-288-4440;

Fax: 001-414-288-713;

Email: pgrover@mcw.edu

Carolyne Albert, Ph.D. : Orthopaedic and Rehabilitation Engineering Center, Marquette University, ASF, Suite 105, 735 N. 17th St, PO Box 1881, Milwaukee, WI 53201-1881, USA

Mei Wang, Ph.D. : Orthopaedic and Rehabilitation Engineering Center, Marquette University, ASF, Suite 105, 735 N. 17th St, PO Box 1881, Milwaukee, WI 53201-1881, USA

Journal of Engineering in Medicine Proceedings of the Institution of Mechanical Engineers, Part H, Vol. 225, No. 12 (December 2011): pg. 1169-1176. DOI.

Gerald F. Harris, Ph.D., P.E. : Orthopaedic and Rehabilitation Engineering Center, Marquette University, ASF, Suite 105, 735 N. 17th St, PO Box 1881, Milwaukee, WI 53201-1881, USA

Journal of Engineering in Medicine Proceedings of the Institution of Mechanical Engineers, Part H, Vol. 225, No. 12 (December 2011): pg. 1169-1176. DOI.